Available online at www.sciencedirect.com
SCIENCE DIRECT®
Journal of Magnetic Resonance 175 (2005) 11–20
JMR Journal of Magnetic Resonance
www.elsevier.com/locate/jmr

Homo-nuclear ^{13}C *J*-decoupling in uniformly ^{13}C-enriched solid proteins

Tatyana I. Igumenova [1], Ann E. McDermott *

Department of Chemistry, Columbia University, 3000 Broadway MC 3113, New York, NY 10027, USA

Received 10 November 2004; revised 28 February 2005
Available online 5 April 2005

Abstract

Recently, we reported an analysis of carbon lineshapes in high resolution solid-state NMR spectra of uniformly ^{13}C-enriched amino acids. Application of a ^{13}C *J*-decoupling protocol during the carbon chemical shift evolution period allowed us to separate the contribution of the second-order dipolar shift from that of the ^{13}C–^{13}C *J*-coupling interactions to carbon linewidths. In this work, we have extended this approach to microcrystalline proteins. We describe the performance of the *J*-decoupling sequence applied to remove homo-nuclear ^{13}C *J*-couplings in the ^{13}C spectra of ubiquitin. Analysis of the *J*-decoupling efficiency for Cα and carbonyl protein sites showed that a significant gain in resolution can be achieved.

Keywords: Solid-state NMR; Microcrystalline protein; Spectral assignment; Magic angle spinning; *J*-decoupling.

1. Introduction

Good resolution and signal-to-noise are essential for the successful assignment of multidimensional NMR spectra of proteins. One of the means to improve resolution and sensitivity in solution NMR spectra is to remove the homo-nuclear and hetero-nuclear *J*-coupling interactions in the indirect dimensions [1–6]. Recently, it has become clear that with the development of sample preparation protocols, where hydration of proteins is preserved and conformational heterogeneity is minimized [7,8], solid-state NMR could benefit from *J*-decoupling protocols as well. With the typical free precession ^{13}C linewidths of 0.5–1.0 ppm [7], removal of homo-nuclear ^{13}C *J*-coupling interactions (55 Hz for Cα–CO, 35 Hz for Cα–Cβ [9]) could substantially reduce ^{13}C linewidths at moderate and high magnetic field strengths.

For uniformly ^{13}C-enriched solid amino acids and proteins, Straus et al. [10,11] proposed a *J*-decoupling scheme that removes the interaction in the indirect dimension. The method is based on the combination of hard and selective π-pulses placed in the middle of the carbon chemical shift evolution period. An alternative way of removing *J*-decoupling interactions was proposed recently based on a solid-state variant of the solution "In-Phase-Anti-Phase" experiment [12,13].

Recently [14], we have characterized the contribution of the second-order dipolar shift [15,16] to ^{13}C linewidths in amino acids using *J*-decoupling as a means to separate the dipolar and *J*-coupling interactions. Our *J*-decoupling scheme was very similar to that reported by Straus et al. [10,11], but made use of the transverse DANTE pulse applied on-resonance for the detected spin. In this work, the same decoupling scheme was applied to uniformly ^{13}C,^{15}N-enriched ubiquitin. The main goal of the protein study was to investigate whether an improvement of spectral resolution achieved

* Corresponding author. Fax: +1 212 932 1289.
E-mail address: aem5@columbia.edu (A.E. McDermott).
[1] Present address: Department of Biochemistry and Biophysics, University of Pennsylvania, Philadelphia, PA 19104, USA.

1090-7807/$ - see front matter © 2005 Elsevier Inc. All rights reserved.
doi:10.1016/j.jmr.2005.03.007

by *J*-decoupling would be sufficient to carry out at least part of the resonance assignment work at moderate applied magnetic field strength.

One motivation for working at moderate magnetic field strength, 9.4 T (400 MHz ^{1}H frequency), was the issue of protein sample stability. Excellent chemical shift dispersion of protein spectra at high magnetic fields is to a certain extent counter-balanced by the heating effects due to high magic angle spinning (MAS) frequencies and strong radio-frequency fields. Radio-frequency sample heating and the associated loss in the probe quality factor are significant only for conductive NMR samples. Microcrystalline formulations of uniformly ^{13}C-enriched ubiquitin used in our experiments contain mother liquor, which is conductive due to the presence of a 20 mM buffer solution. For electrically conductive samples, two types of radio-frequency losses were identified, inductive and dielectric [17,18], that scale as the fourth and third power of the excitation frequency, respectively. Excessive heating due to high speed spinning and/or RF irradiation could cause protein aggregation and unfolding at high applied magnetic fields, so in cases of protein samples in high ionic strength it could be advantageous to carry out NMR experiments at moderate magnetic field strengths.

In this work, we recorded a set of two-dimensional (2D) ^{13}C–^{15}N chemical shift correlation spectra for a microcrystalline formulation of uniformly ^{13}C,^{15}N-enriched ubiquitin at 9.4 T. The ^{15}N nucleus was used for direct detection, while the *J*-decoupling of ^{13}C-enriched protein sites was carried out in the indirect dimension of the 2D spectra. Analysis of the resolved cross-peaks in the CON spectra (correlating the ^{15}N chemical shift of amide groups with that of the preceding carbonyl ^{13}C) showed that the second-order dipolar shift manifested itself in the characteristic free precession and *J*-decoupled carbonyl lineshapes. Line broadening due to the dipolar shift was also detected for Cα protein sites. *J*-decoupling did improve the resolution in CON ubiquitin spectra at two spinning frequencies, 5 and 9 kHz, and in CαN spectra (correlating the ^{15}N chemical shift of amide groups with that of the intra-residue ^{13}Cα) at 9 kHz. The quantitative criteria for such an improvement were (i) the difference between free precession and *J*-decoupled linewidths and (ii) the relative number of resolved ^{13}C–^{15}N cross-peaks in free precession and *J*-decoupled spectra.

Signal retention in *J*-decoupling experiments was estimated by comparing the volumes of cross-peaks in the free precession and decoupled spectra at a spinning frequency of 9 kHz. Average signal retention for all resolved cross-peaks was found to be lower than for a model compound, alanine. Nevertheless, signal-to-noise ratios of individual cross-peaks in free precession and decoupled spectra were comparable. In accordance with the model compound findings, *J*-decoupled CON protein spectra at a spinning frequency of 5 kHz showed spectral resolution superior to that observed at 9 kHz. However, the sensitivity of the 5 kHz spectra suffered from the effects of non-negligible chemical shift anisotropy of ^{13}CO sites. The signal-to-noise ratios of individual cross-peaks at 5 kHz were on average smaller compared to their 9 kHz counterparts.

2. Results

2.1. Effect of ^{13}C *J*-decoupling on the spectra of ^{13}CO protein backbone sites

Two-dimensional CON chemical shift correlation spectra of ubiquitin were collected using the selective double cross-polarization pulse sequence. Every 2D spectrum was a sum of three individual experiments, 13 h each, and thus has a total duration of 39 h. *J*-decoupled spectra and free precession spectra were collected with a π pulse on the ^{15}N channel in the middle of t_1 evolution period to eliminate the contribution of the hetero-nuclear *J*-couplings to the linewidth. Two spinning frequency regimes, 9 and 5 kHz, were explored.

Fig. 1 shows a comparison of the free precession (A) and *J*-decoupled (B) CON spectra collected at a spinning frequency of 9 kHz and processed identically, including the resolution enhancement in t_1 (a 60° sine bell function). The duration of the selective pulse was four rotor periods or 444.44 μs at 9 kHz. The total evolution time in t_1 was 21.3 ms. The assignment of cross-peaks was carried out based on a set of 3D experiments reported elsewhere [19,20]. From a cursory inspection of Fig. 1, it is clear that considerable resolution improvement is observed in the *J*-decoupled spectrum. Twenty-eight cross-peaks could be clearly identified in the *J*-decoupled spectrum. Degenerate cross-peaks and cross-peaks that are not completely resolved in the free precession spectrum were not used for quantitative analysis of *J*-decoupling. Table 1 shows assignments and signal-to-noise ratios of the 17 cross-peaks used in the subsequent quantitative analysis of the *J*-decoupling performance.

2.2. Low versus high spinning frequency

One way to eliminate the inhomogeneous line broadening originating from the second-order dipolar shift is to move further away from the $n = 1$ rotational resonance condition for the CO–Cα pair, which can be done by changing the spinning frequency. We found that carbonyl linewidths as narrow as 36 Hz can be obtained using a spinning frequency of 5 kHz for uniformly enriched alanine [14]. Fig. 1 shows a comparison of *J*-decoupled ubiquitin spectra collected at 9 kHz (B) and 5 kHz (C). The contour threshold for the 5 kHz spec-

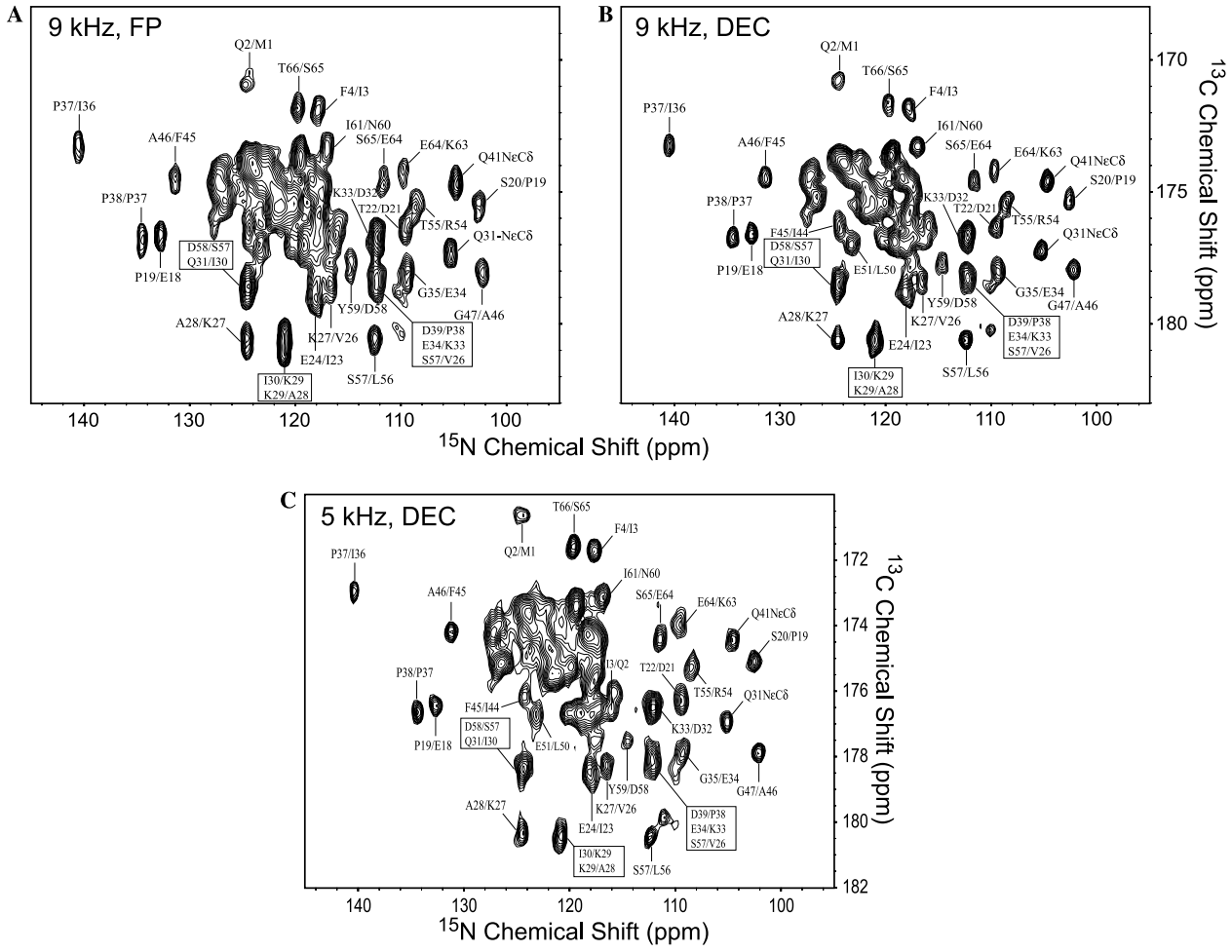

Fig. 1. 2D CON free precession (A) and *J*-decoupled (B, C) double cross-polarization spectra of uniformly enriched ubiquitin. The spectra were recorded at spinning frequencies of 9 kHz (A, B) and 5 kHz (C). The cross-peaks were assigned based on 3D experiments reported elsewhere [19,20]. The *J*-decoupling protocol produces significant resolution enhancement in the protein spectra at both spinning frequencies.

Table 1
Assignments, resonance positions, and signal-to-noise ratios for all cross-peaks used for the determination of linewidth reduction and signal retention in three 2D CON correlation spectra recorded at a spinning speed of (i) 9 kHz, free precession; (ii) 9 kHz, decoupled; and (iii) 5 kHz, decoupled

Cross-peak	^{15}N (ppm)	^{13}C (ppm)	Signal-to-noise ratio[a]		
			9 kHz, free precession	9 kHz, decoupled	5 kHz, decoupled
Gln41Nε2–Cδ[b]	104.6	174.6	25	26	15
Gln31Nε2–C[b]	105.2	177.2	17	22	15
Gln2N–Met1CO	124.5	170.7	7	11	11
Phe4N–Ile3CO	117.8	171.8	16	15	16
Pro19N–Glu18CO	132.7	176.6	19	20	15
Ser20N–Pro19CO	102.6	175.3	12	13	16
Ala28N–Lys27CO	124.5	180.6	19	19	14
Gly35N–Glu34CO	109.4	178.0	21	17	13
Pro37N–Ile36CO	140.4	173.1	15	15	10
Pro38N–Pro37CO	134.4	176.7	18	17	18
Ala46N–Phe45CO	131.3	174.4	16	14	14
Gly47N–Ala46CO	102.2	178.0	17	17	14
Ser57N–Leu56CO	112.4	180.5	21	19	15
Tyr59N–Asp58CO	114.6	177.7	13	16	10
Ile61N–Asn60CO	116.9	173.2	16	20	20
Ser65N–Glu64CO	111.5	174.5	10	18	15
Thr66N–Ser65CO	119.7	171.7	22	15	15

[a] Signal-to-noise ratio was determined using Sparky software [19].
[b] Side-chain resonances (Cδ) of glutamine residues.

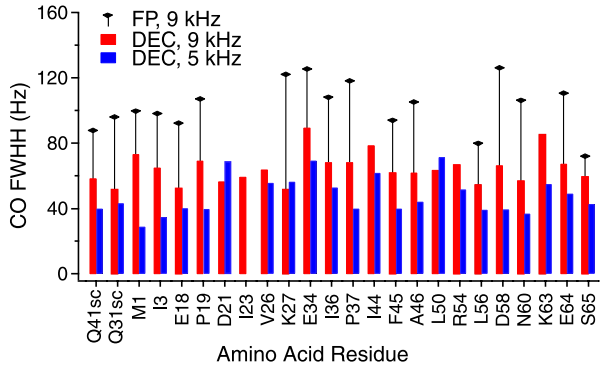

Fig. 2. Carbonyl linewidths determined in free precession and *J*-decoupled 2D CON spectra. *J*-decoupled spectra were collected at two spinning frequencies, 5 kHz (blue bars) and 9 kHz (red bars). The missing bars correspond to the resonances that are either unresolved or have very low intensities. The narrowest linewidths are obtained when *J*-decoupling protocol is applied in the low spinning frequency regime (5 kHz).

trum was adjusted proportionally to the average difference in peak heights between the individual cross-peaks at 5 and 9 kHz. The duration of the selective pulse at 5 kHz was two rotor periods or 400 μs. The maximum evolution time in the indirect dimension was 19.2 ms. The total number of 2D points was identical for the 5 and 9 kHz experiments.

From the 2D spectra of Fig. 1 it is clear that several spectral regions in the 5 kHz spectrum are better resolved than in the 9 kHz spectrum. Carbonyl linewidths measured in unapodized spectra at 5 kHz are shown in Fig. 2 with blue bars. For the majority of cross-peaks, narrower lines are obtained at 5 kHz, which is in total agreement with our results on a model compound [14]. For the cross-peaks resolved in the free precession spectra, the average free precession carbonyl linewidth was 103 Hz, and the average *J*-decoupled linewidths were 63 Hz at 9 kHz and 43 Hz at 5 kHz. The signal-to-noise ratios of individual cross-peaks presented in Table 1 are in general lower at 5 kHz than at 9 kHz. While the spectral resolution definitely improves at lower spinning frequencies, signal loss due to the chemical shift anisotropy of carbonyl sites becomes substantial, leading to a decrease in sensitivity.

2.3. Effect of *J*-decoupling on the spectra of $^{13}C\alpha$ protein backbone sites

Two-dimensional CαN chemical shift correlation spectra of uniformly enriched ubiquitin were collected using approximately the same parameters as those for CON, except that the ^{1}H–^{13}C contact time was kept very short (100 μs) to preferentially build up the Cα polarization. For *J*-decoupling experiments, the duration of the selective pulse was six rotor periods, or 666.67 μs at 9 kHz.

While a Gaussian pulse of a very large bandwidth and, as a consequence, flat inversion profile over the chemical shift range of interest can be used for the decoupling of carbonyl sites, this is not the case for Cα. The Cβ chemical shift region partially overlaps with Cα, making efficient Cα–Cβ decoupling difficult. Thus, for a Gaussian-shaped inversion profile, one has to find a compromise between bandwidth and decoupling efficiency. In our experiments, the carrier frequency of the selective pulse was set to 57 ppm. The most "problematic" amino acids were glycines, with Cα offset of 11 ppm or 1.1 kHz, threonines, with Cβ offset of 13 ppm or 1.3 kHz, and serines, with Cβ offset of 7 ppm or 0.7 kHz. Checking these offsets against the Cα/Cβ inversion profile presented in Fig. 5(B), we conclude that, as a result of selective inversion, (i) around 40% of the glycine signal will be retained, and (ii) partial or no Cα–Cβ decoupling will be observed for threonines and serines, respectively. More sophisticated pulse shapes with superior inversion profiles, such as, e.g., REBURP [21], can be used to alleviate the problem of Cα/Cβ decoupling, provided that the duration of the selective pulse is kept short compared to ^{13}C T_2 and the solid-state NMR spectrometer has adequate pulse-shaping capabilities.

CαN experiments were not carried out at a spinning frequency of 5 kHz. The experiments on alanine showed that no sensitivity gain is expected at 5 kHz due to the presence of Cα–Cβ dipolar coupling interactions. Moreover, the requirement of applying the selective pulse on a rotational echo imposes a limitation on the spectral width in the indirect dimension. At 5 kHz, the spectral width would be smaller than the Cα chemical shift dispersion.

Fig. 3 shows a comparison of the free precession (A) and *J*-decoupled (B) spectra collected at a spinning frequency of 9 kHz and processed with the same resolution enhancement in t_1. The maximum evolution time in t_1 dimension was 21.3 ms. The assignment of cross-peaks was carried out based on a set of 3D experiments reported in [19,20]. As in the case of the carbonyl sites, it is clear that a considerable resolution improvement is observed in the *J*-decoupled spectrum. Thirty cross-peaks can be identified in the displayed region of the *J*-decoupled spectrum. Seventeen of them are sufficiently well resolved in the free precession spectrum and appear to be suitable for quantitative analysis. The assignments and signal-to-noise ratios for all cross-peaks that were used in the subsequent quantitative analysis of the *J*-decoupling performance are presented in Table 2.

2.4. Carbonyl lineshapes in free precession and decoupled spectra

Fig. 4 shows several cross-sections through the ^{15}N dimension of the free precession (spinning frequency

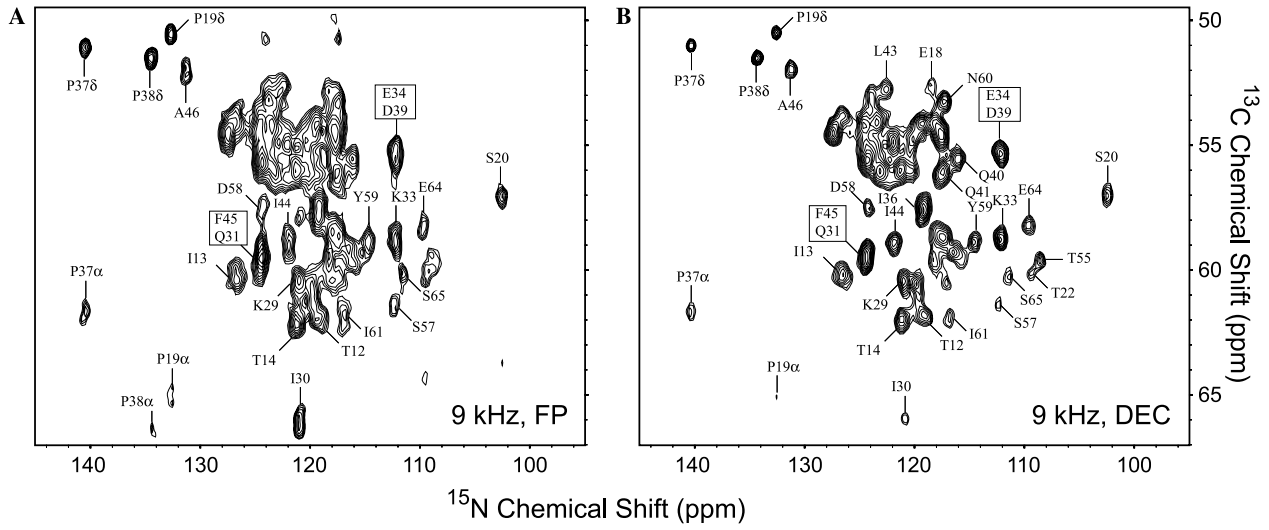

Fig. 3. 2D CαN free precession (A) and *J*-decoupled (B) double cross-polarization spectra of uniformly enriched ubiquitin recorded at a spinning frequency of 9 kHz. The cross-peaks were assigned based on 3D experiments reported elsewhere [19,20]. Proline cross-peaks have lower intensities compared to those of other amino acids due to the low efficiency of the first ^{1}H–^{15}N cross-polarization step. The *J*-decoupling protocol produces significant resolution enhancement in the protein spectrum.

Table 2
Assignments, resonance positions, and signal-to-noise ratios for all cross-peaks used for the determination of linewidth reduction and signal retention in two 2D CαN correlation spectra recorded at a spinning frequency of 9 kHz

Cross-peak	^{15}N (ppm)	^{13}C (ppm)	Signal-to-noise ratio[a]	
			9 kHz, free precession	9 kHz, decoupled
Ile13N–Cα	126.7	59.9	13	18
Thr14N–Cα	121.3	61.8	20	20
Pro19N–Cα	132.8	64.8	6	8
Pro19N–Cδ	132.7	50.3	17	17
Ser20N–Cα	102.6	56.8	14	15
Ile30N–Cα	121.1	65.8	14	9
Lys33N–Cα	112.3	58.5	18	25
Pro37N–Cα	140.6	61.4	11	10
Pro37N–Cδ	140.5	50.8	16	16
Pro38N–Cδ	134.6	51.3	20	22
Ile44N–Cα	122.0	58.7	16	19
Ala46N–Cα	131.4	51.7	10	14
Asp58N–Cα	124.4	57.3	11	14
Tyr59N–Cα	114.8	58.6	13	18
Ile61N–Cα	117.0	61.7	11	9
Glu64N–Cα	109.8	58.0	11	15
Ser65N–Cα	111.6	59.9	12	11

[a] Signal-to-noise ratio was determined using Sparky software [19].

9 kHz) and *J*-decoupled spectra (9 and 5 kHz). To facilitate the lineshape analysis, the t_1 dimension was zero-filled four times and processed without apodization. Free precession carbonyl resonances of Met1, Pro37, and Phe45 (left column) have asymmetric triplet-like lineshapes, while the decoupled lineshapes of Met1 and Phe45 (center column) at 9 kHz are clear powder patterns of second-order dipolar shifts. ^{13}C cross-sections of the *J*-decoupled spectrum collected at 5 kHz are shown in the right column of Fig. 4. The difference in *J*-decoupled lineshapes and linewidths (see Fig. 2) that we observe for the two spinning frequencies is entirely due to the residual ^{13}C–^{13}C dipolar couplings present at 9 kHz.

2.5. Signal retention in J-decoupling experiments

To evaluate the performance of the *J*-decoupling protocol, it is important to know how much signal is left after the application of the *J*-decoupling sequence. The following procedure was employed to analyze signal retention in protein spectra: for every resolved cross-peak, we measured the corresponding volume in each of three separate experiments contributing to the final 2D spectrum. From these three measurements, we calculated the mean cross-peak volumes and their standard deviations. The uncertainty in cross-peak volumes is mainly determined by the spectral noise and instrumental instabilities that influence the transfer efficiency in 2D experiments. Doing three repetitive integrations of the *same* 2D spectrum allowed us to assess the precision of the integration procedure, which was found to be better than 2% for all cross-peaks. For each cross-peak, signal retention was calculated as a ratio of the cross-peak volume obtained in the *J*-decoupled experiment to that in the free precession experiment. The uncertainty of the ratio was derived from the uncertainty of two volumes.

Fig. 5 shows the dependence of signal retention on the carrier offset for all resolved ^{13}CO (A) and Cα (B) cross-peaks in the free precession spectrum. Dashed lines represent the inversion profile of the corresponding center-bands of alanine. In both cases, the experimental

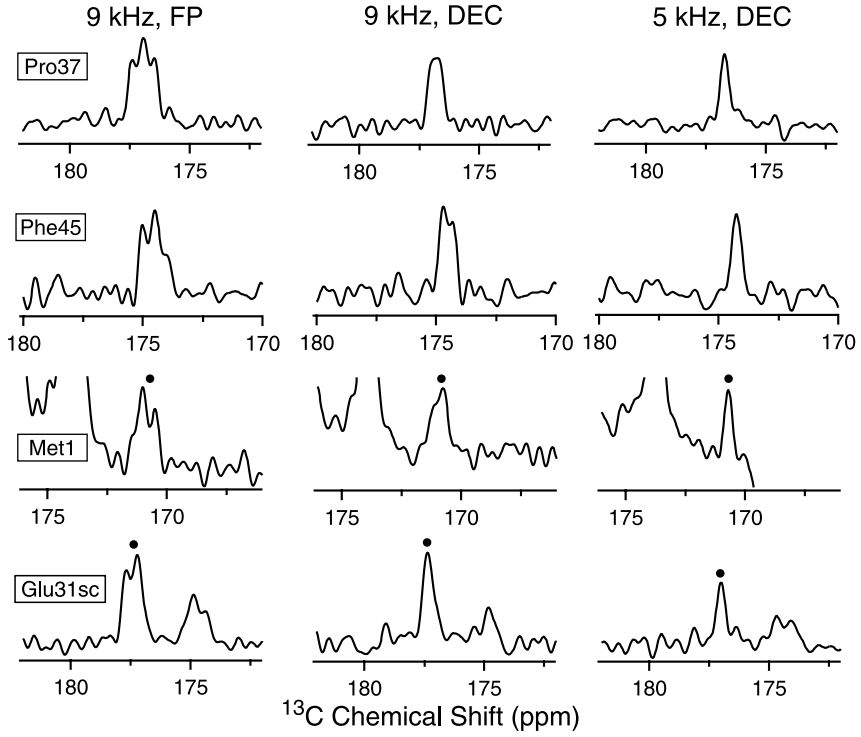

Fig. 4. Free precession and *J*-decoupled carbonyl lineshapes for several resolved cross-peaks in ubiquitin. The cross-sections were taken through the ^{15}N chemical shift corresponding to the next residue in the sequence. The vertical scale is identical for every trio of free precession/*J*-decoupled cross-sections. A combination of second-order dipolar shift and *J*-coupling produces triplet-like free precession lineshapes for the carbonyl atoms (left column). Removal of *J*-coupling interaction gives rise to powder patterns of second-order dipolar shifts at 9 kHz (center column) and ^{13}C singlets at 5 kHz (right column). A notable exception is the Glu31 side-chain that has a doublet-like lineshape in its free precession spectra at 9 kHz (see text for details).

data points essentially follow the alanine profile, although the actual signal retention values are somewhat lower compared to the model compound, presumably due to the existence of additional relaxation pathways in the protein.

2.6. Reduction of linewidths

The observed reduction of carbonyl linewidths afforded by *J*-decoupling is calculated as a difference between the free precession and decoupled linewidths. It is plotted in Fig. 6 as a function of amino acid residue (A) and carrier offset (B). Inspection of Fig. 6B allows one to conclude that there is no correlation between the *J*-decoupling efficiency and the carrier offset. The lack of correlation seems to be plausible, since the inversion profile of the selective pulse is rather flat. Two outliers with abnormally low and high values of linewidth reduction are Ser65 and Lys27, respectively. The reason is the distorted triplet- and doublet-like lineshapes for these amino acids. Possible origins of the lineshape distortion will be addressed in Section 3. Similar plots for the free precession and *J*-decoupled Cα linewidths are presented in Fig. 7. Very small linewidth reduction, around 15 Hz, is observed for serines and threonines, presumably due to the incomplete Cα–Cβ *J*-decoupling.

3. Discussion

^{13}C *J*-decoupling was applied to remove homo-nuclear ^{13}C couplings in the indirect dimension of 2D ^{13}C–^{15}N chemical shift correlation spectra of ubiquitin. Below, we discuss the efficiency of *J*-decoupling using signal retention, reduction of linewidths, and signal-to-noise ratios as major criteria. We also compare the carbonyl lineshapes of individual cross-peaks at two different spinning frequencies, 5 and 9 kHz.

As reported previously by two groups [14,22], at a spinning frequency of 9 kHz, the second-order dipolar shift gives rise to inhomogeneous broadening of the CO and Cα resonances. For uniformly ^{13}C-enriched alanine, the dipolar broadening (53 Hz) is comparable with the CO–Cα *J*-coupling constant. We showed experimentally and computationally that the decoupled lineshape is a powder pattern of second-order dipolar shifts. When combined with homo-nuclear *J*-coupling interactions, the carbonyl resonance acquires a characteristic triplet-like lineshape. In contrast, at 5 kHz, the contribution of the residual ^{13}C dipolar couplings to the lineshape is negligible, producing a single line in the *J*-decoupled spectrum. We found that carbonyl lineshapes in solid-state NMR spectra of ubiquitin follow the same pattern.

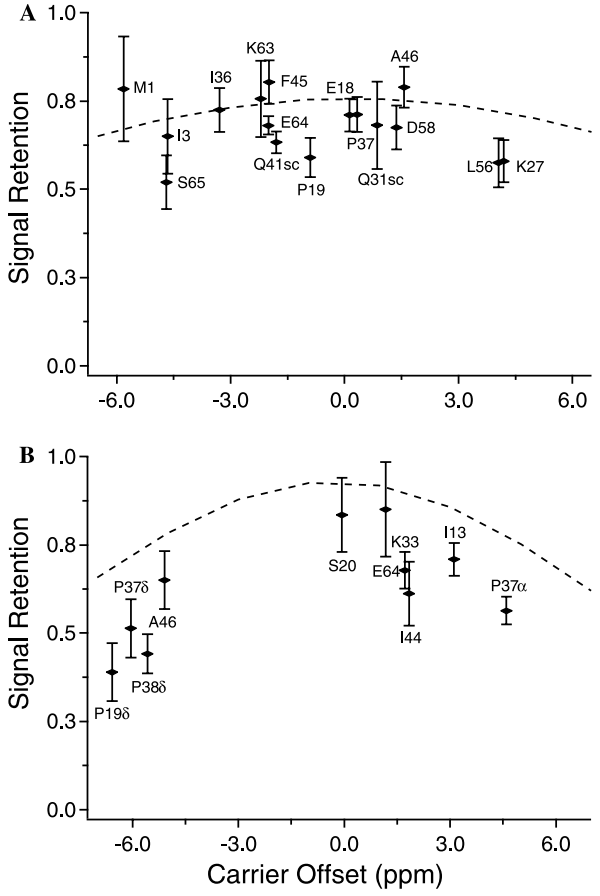

Fig. 5. Signal retention in *J*-decoupled (A) CON and (B) CαN experiments plotted as a function of the carbon carrier offset. The signal retention was calculated as, V_{DEC}/V_{FP} where V_{DEC} and V_{FP} are the cross-peak volumes for a given amino acid. The inversion profiles of alanine Cα and CO carbons are shown with the dashed line. The duration of the selective pulse was 6 rotor periods, or 666.67 μs, for Cα, and 4 rotor periods, or 444.4 μs, for CO. The average signal retention is 68 and 62% for the CO and Cα carbons, respectively.

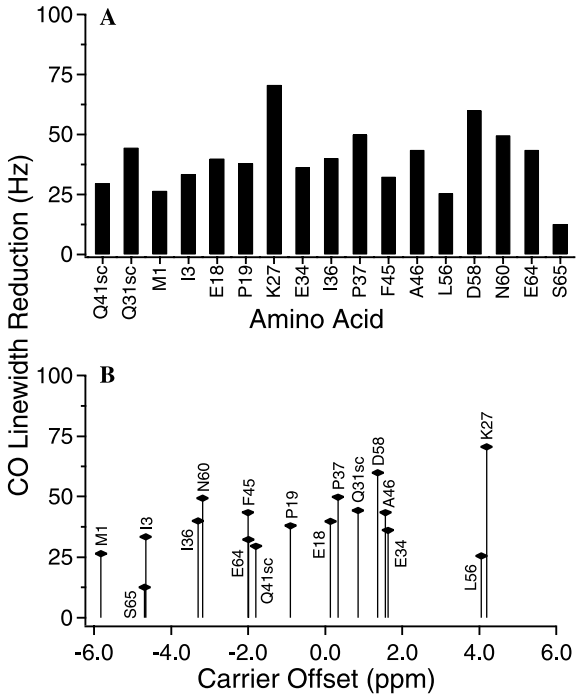

Fig. 6. ^{13}CO reduction of linewidth, calculated as a difference between the free precession and decoupled linewidths, as a function of (A) amino acid residue and (B) carbon carrier offset. As a result of *J*-decoupling, the average CO linewidth is reduced by 39% or 40 Hz (0.40 ppm at 9.4 T).

For all cross-peaks listed in Table 1, with the exception of glutamine side-chains, we observed triplet-like free precession lineshapes (see Fig. 4). Free precession Cδ resonance of Glu31 side-chain is almost entirely dominated by *J*-coupling interactions. This is because the Cδ–Cγ spin pair with the chemical shift difference of ~145 ppm, is far above the rotational resonance condition at 9 kHz. Resolved powder patterns of second-order dipolar shifts are seen in some of the *J*-decoupled lineshapes, such as Phe45 (Fig. 4, center column). In the majority of cases, however, the second-order dipolar shift is less obvious and is obscured presumably due to some other line broadening mechanism. To our knowledge, this is the first time that the fine structure of protein carbonyl resonances, resulting from a combination of the second-order dipolar shift and *J*-coupling interactions, is reported. In the low spinning frequency regime, the contribution of residual ^{13}C–^{13}C dipolar couplings to the linewidth is negligible, and the *J*-decoupling pro-

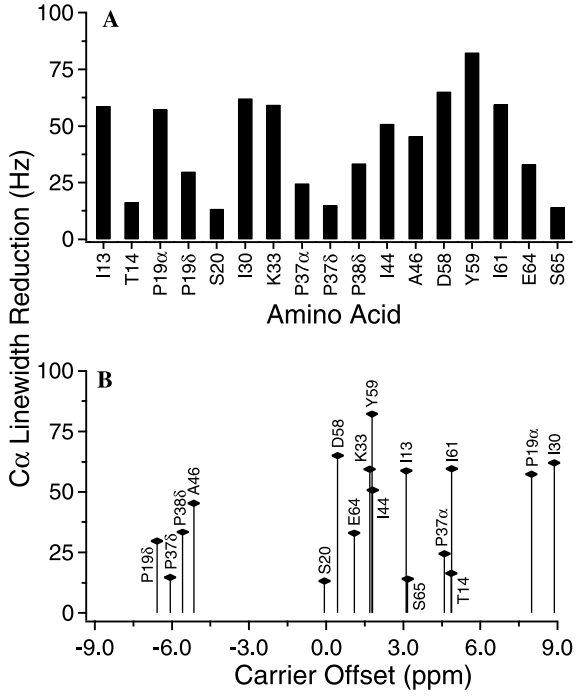

Fig. 7. ^{13}Cα reduction of linewidth, calculated as a difference between the free precession and decoupled linewidths, as a function of (A) amino acid residue and (B) carbon carrier offset. As a result of *J*-decoupling, the average Cα linewidth is reduced by 40% or 42 Hz (0.42 ppm at 9.4 T).

tocol produces single lines devoid of any fine structure (Fig. 4, right column). This finding indicates that low spinning frequency regime could be useful for proteins with limited ^{13}C chemical shift dispersion such as α-helical membrane proteins.

In our previous work [14], we discussed the influence of non-negligible chemical shift anisotropy on the performance of the decoupling pulses. At a spinning frequency of 9 kHz, we obtained signal retention of 78% for the carboxyl carbon and almost complete signal recovery for the Cα carbon in uniformly ^{13}C-enriched alanine. Fig. 5 shows that the signal retention values are somewhat lower for the carbons of protein backbone. The average signal retention in ubiquitin (calculated using cross-peak volumes as described in Section 2) is 68 and 62% for the CO and Cα carbons, respectively. We speculate that the origin of the signal loss in the *J*-decoupled protein spectra is probably associated with the relaxation losses during the selective pulse.

A comparison of signal-to noise ratios calculated based on the peak intensities in free precession and *J*-decoupled spectra (Tables 1 and 2) indicates that the sensitivity enhancement is relatively modest for both backbone carbons, although signal-to-noise ratios are generally higher for the *J*-decoupled cross-peaks at 9 kHz. This means that the reduced total signal is essentially compensated for by line narrowing due to the *J*-decoupling. Thus, it is mainly the resolution enhancement that warrants the use of *J*-decoupling in protein experiments. As reported previously by Straus et al. [11], a signal-to-noise gain of ~1.5 could be obtained if ^{13}C direct detection is used instead of ^{15}N. Inspection of Tables 1 and 2 shows that, for the spinning frequency of 9 kHz, the ratio of *J*-decoupled and free precession signal-to-noise ratios is larger than 1 for 11 carbonyl and 13 Cα cross-peaks. Combined with superior resolution of the nitrogen dimension, the ^{15}N-detected experiments with *J*-decoupling in the carbon dimension represent a viable alternative to the direct ^{13}C detection.

Comparison of *J*-decoupled carbonyl data (Table 1) shows that the signal-to-noise ratios in the 5 kHz experiment are less than or comparable to those in the 9 kHz experiment. Since the length of the selective pulse is approximately the same in the two experiments, it is valid to assume that the relaxation losses during the selective pulses are identical. If one takes into account only the differences in the experimental parameters, such as the number of scans per t_1 point and the total number of t_1 points, the signal-to-noise ratio in the 9 kHz experiment should be ~13% higher than that in the 5 kHz experiment. The differences that we observe in the signal-to-noise ratios for the two spinning frequencies are mostly due to the effect of non-negligible CSA at the spinning frequency of 5 kHz on the average signal amplitude.

The reduction in ^{13}C linewidths vs. residue number in the amino acid sequence and carrier offset is plotted in Figs. 6 and 7. The linewidths were determined automatically by Sparky software [23] (using t_1-unapodized 2D spectra) and should be treated as estimates only. An accurate measurement of linewidths would require individual fitting of each cross-peak, due to their complex lineshape in the carbon dimension. The combined effect of (i) the orientation dependence of the polarization transfer sequence [14], (ii) the kinetics of polarization transfer, and (iii) the reduced signal-to-noise ratios in protein spectra could produce distortions in the triplet-like lineshapes that might lead to over- and under-estimation of true linewidths. The average value of linewidth reduction for carbonyl carbons was found to be 40 Hz, or 0.40 ppm at 9.4 T (Fig. 6A). For the Cα, the average linewidth reduction was found to be 42 Hz, which makes up 40% of the average free precession Cα linewidth (Fig. 6B). For both backbone carbons, the reduction in linewidth appears to be largely independent of the carrier offset (Figs. 6B and 7B). It is useful to compare *J*-decoupled solid-state NMR linewidths of backbone carbons with those obtained in solution NMR experiments with constant-time ^{13}C evolution periods. The constant time delays are usually set to tens of milliseconds giving the digital resolution of the same order as the carbon linewidths that we obtained in the *J*-decoupled solid-state NMR experiments (Fig. 2).

In summary, we found that *J*-decoupling at a spinning frequency of 9 kHz resulted in an enhancement of spectral resolution, but not sensitivity. The average linewidth reduction was found to be 40 Hz for ^{13}CO and 42 Hz for Cα protein sites, which makes up 40% of the free precession carbon linewidths. Lowering the spinning frequency to 5 kHz in conjunction with *J*-decoupling provided further resolution enhancement, resulting in the reduction of ^{13}CO linewidths by 58%. In the low spinning frequency regime one should expect some signal loss due to the non-negligible chemical shift anisotropy of the protein carbonyl sites.

4. Conclusions

In this work, we demonstrated that *J*-decoupling improves the resolution of the carbon dimension in the spectra of microcrystalline uniformly ^{13}C-enriched proteins. The performance of this pulse sequence for ubiquitin was remarkably similar to the results obtained for a model compound, alanine [14]. At a spinning frequency of 9 kHz, second-order dipolar shift makes a significant contribution to the carbon linewidths of the protein backbone atoms. For carbonyl sites, the dipolar shift combined with *J*-coupling interactions, gives rise to characteristic triplet-like lineshapes. Triplet- and doublet-like lineshapes, the latter obtained as a result of *J*-decoupling were detected for several amino acid residues.

J-decoupling experiments at 9 kHz invariably led to resolution enhancement in the carbon dimension. Sensitivity gain is noticeable for Cα and negligible for CO sites due to the large chemical shift anisotropy of the latter. At a spinning frequency of 5 kHz, the contribution of ^{13}C–^{13}C dipolar coupling interactions to the linewidths is negligible, giving the average carbonyl linewidth of 43 Hz, or 0.43 ppm. In this case, the resolution enhancement is accompanied by signal loss due to the chemical shift anisotropy.

J-decoupling protocols in solid-state NMR are useful if *J*-coupling interactions make a dominant contribution to the carbon linewidths. This is the case for microcrystalline protein formulations and protein samples prepared by a well-controlled precipitation. If the some signal loss is tolerable, further resolution enhancement in the indirect dimension can be achieved at low spinning frequencies.

5. Materials and methods

Uniformly ^{13}C,^{15}N-enriched ubiquitin was a generous gift of Professor A. Joshua Wand (University of Pennsylvania). The level of isotope enrichment was >99% for both nuclei. About 15 mg of uniformly ^{13}C,^{15}N-enriched ubiquitin was crystallized by batch methods in 60% 2-methyl-2,4-pentanediol (MPD), 20 mM citrate buffer, pH 4.0–4.2.

5.1. NMR experiments

All solid-state NMR experiments were carried out on a 400 MHz Infinity Plus NMR spectrometer equipped with a 4 mm T3 MAS probe (Varian/Chemagnetics). The spinning frequency was controlled with an accuracy of ±3 Hz. The pulse sequence used in the experiments is described elsewhere [14]. In brief, 2D selective double cross-polarization (DCP) experiments [24] were performed in order to record the CON and CαN 2D spectra of ubiquitin. Based on our *J*-decoupling results for a model compound alanine [14], we concluded that, for the carbonyl carbon, the use of relatively low spinning frequency, 5 kHz, could be advantageous in that it provides a better spectral resolution. However, the non-negligible chemical shift anisotropy at this spinning frequency resulted in an appreciable signal loss. To evaluate the feasibility of using low spinning frequencies for the spectroscopy of proteins, we recorded the *J*-decoupled spectrum of ubiquitin at 5 kHz. ^{13}C–^{15}N zero quantum transfers were carried out with the following field strength parameters: ^{15}N 17.5 kHz and ^{13}C 22.5 kHz at 5 kHz spinning frequency; ^{15}N 13.5 kHz and ^{13}C 22.5 kHz at 9 kHz spinning frequency. The DCP transfer efficiencies, determined as the ratio of the intensity of the DCP-filtered ^{15}N signal to the direct ^{15}N cross-polarization signal, were typically 30–40%. TPPM ^{1}H decoupling [25] field strength of 83 kHz and CW field strength of 92 kHz were used during evolution and mixing, respectively. Every 2D experiment represents a sum of three identical 2D experiments, 13 h each, giving a total duration of 39 h. The summation of the individual spectra was carried out in the time domain. Collecting the data in three separate experiments rather than in one longer experiment was done in order to obtain an estimate of the uncertainties in the cross-peak volumes. The uncertainties were calculated as standard deviations of the mean cross-peak volumes.

ω_1-decoupling was carried out using a pair of hard and selective π-pulses in the middle of the evolution period [10,14]. The selective pulse was a transverse DANTE pulse train [26], modulated by a Gaussian function with a 5% truncation amplitude. To minimize the effect of pulse transients, a pair of pulses with a 180° phase shift was substituted for each pulse in the DANTE sequence [27]. The selective pulse and the receiver were phase-cycled according to the spin pinging sequence [28], which ensured the subtraction of signals originating from the out-of-band spins. The total length of the DANTE sequence was adjusted according to the bandwidth requirement for a given spin type. Rotor-synchronization of the indirect dimension sampling and the decoupling element was essential for obtaining artifact-free spectra.

5.2. Data processing and analysis

Cross-peak volumes in 2D spectra were measured using FELIX (Accelrys, San Diego, CA) software. Three different processing schemes were applied to the t_1 dimension of protein spectra: (i) for general two-dimensional contour representation, resolution enhancement by the 60° phase-shifted sine bell functions was used; (ii) for lineshape analysis, the t_1 dimension was zero-filled four times and no apodization function was applied; and (iii) for cross-peak integration, cosine bell apodization was applied to both dimensions, each of which was zero-filled four times. The precision of the FELIX integration procedure was evaluated from three consecutive integrations performed on the same spectrum. The accuracy of cross-peak volume measurements was determined from a separate integration of the three spectra, contributing to the final sum spectrum. The linewidths for all resolved protein cross-peaks and signal-to-noise ratios in the sum spectra were estimated using Sparky [23].

References

[1] E. Kupce, G. Wagner, Multisite band-selective decoupling in proteins, J. Magn. Reson. Ser. B 110 (1996) 309–312.

[2] H. Matsuo, E. Kupce, H.J. Li, G. Wagner, Increased sensitivity in HNCA and HN(CO)CA experiments by selective C-beta decoupling, J. Magn. Reson. Ser. B 113 (1996) 91–96.
[3] M.A. McCoy, L. Mueller, Coherence quenching induced by frequency-selective homo-nuclear decoupling, J. Magn. Reson. 98 (1992) 674–679.
[4] M.A. McCoy, L. Mueller, Selective shaped pulse decoupling in NMR–homo-nuclear [C-13]carbonyl decoupling, J. Am. Chem. Soc. 114 (1992) 2108–2112.
[5] G.W. Vuister, A. Bax, Measurement of 2-bond and 3-bond proton to methyl-carbon *J*-couplings in proteins uniformly enriched with C-13, J. Magn. Reson. Ser. B 102 (1993) 228–231.
[6] T. Yamazaki, W. Lee, C.H. Arrowsmith, D.R. Muhandiram, L.E. Kay, A suite of triple-resonance NMR experiments for the backbone assignment of N-15, C-13, H-2 labeled proteins with high- sensitivity, J. Am. Chem. Soc. 116 (1994) 11655–11666.
[7] A. McDermott, T. Polenova, A. Bockmann, K.W. Zilm, E.K. Paulsen, R.W. Martin, G.T. Montelione, Partial NMR assignments for uniformly (C-13, N-15)-enriched BPTI in the solid state, J. Biomol. NMR 16 (2000) 209–219.
[8] J. Pauli, B. van Rossum, H. Forster, H.J.M. de Groot, H. Oschkinat, Sample optimization and identification of signal patterns of amino acid side chains in 2D RFDR spectra of the alpha-spectrin SH3 domain, J. Magn. Reson. 143 (2000) 411–416.
[9] J. Cavanagh, W. Fairbrother, A.G. Palmer, N.J. Skelton, in: Protein NMR Spectroscopy: Principles and Practice, Academic Press, 1996, pp. 480–481.
[10] S.K. Straus, T. Bremi, R.R. Ernst, Resolution enhancement by homo-nuclear J decoupling in solid- state MAS NMR, Chem. Phys. Lett. 262 (1996) 709–715.
[11] S.K. Straus, T. Bremi, R.R. Ernst, Experiments and strategies for the assignment of fully C-13/N-15-labelled polypeptides by solid state NMR, J. Biomol. NMR 12 (1998) 39–50.
[12] L. Duma, S. Hediger, B. Brutscher, A. Bockmann, L. Emsley, Resolution enhancement in multidimensional solid-state NMR spectroscopy of proteins using spin-state selection, J. Am. Chem. Soc. 125 (2003) 11816–11817.
[13] L. Duma, S. Hediger, A. Lesage, L. Emsley, Spin-state selection in solid-state NMR, J. Magn. Reson. 164 (2003) 187–195.
[14] T.I. Igumenova, A.E. McDermott, Improvement of resolution in solid state NMR spectra with *J*-decoupling: an analysis of lineshape contributions in uniformly C-13-enriched amino acids and proteins, J. Magn. Reson. 164 (2003) 270–285.
[15] Z.H. Gan, D.M. Grant, Pseudo-spin rotational resonance and homo-nuclear dipolar NMR of rotating solids, Mol. Phys. 67 (1989) 1419–1430.
[16] M.H. Levitt, D.P. Raleigh, F. Creuzet, R.G. Griffin, Theory and simulations of homo-nuclear spin pair systems in rotating solids, J. Chem. Phys. 92 (1990) 6347–6364.
[17] D.G. Gadian, F.N.H. Robinson, Radiofrequency losses in NMR experiments on electrically conducting samples, J. Magn. Reson. 34 (1979) 449–455.
[18] D.I. Hoult, P.C. Lauterbur, Sensitivity of the zeugmatographic experiment involving human samples, J. Magn. Reson. 34 (1979) 425–433.
[19] T.I. Igumenova, A.J. Wand, A.E. McDermott, Assignment of the backbone resonances for microcrystalline ubiquitin, J. Am. Chem. Soc. 126 (2004) 5323–5331.
[20] T.I. Igumenova, A.E. McDermott, K.W. Zilm, R.W. Martin, E.K. Paulsen, A.J. Wand, Assignment of carbon NMR resonances for microcrystalline ubiquitin, J. Am. Chem. Soc. 126 (2004) 6720–6727.
[21] H. Geen, R. Freeman, Band-selective radiofrequency pulses, J. Magn. Reson. 93 (1991) 93–141.
[22] L. Duma, S. Hediger, A. Lesage, D. Sakellariou, L. Emsley, Carbon-13 lineshapes in solid-state NMR of labeled compounds. Effects of coherent CSA-dipolar cross-correlation, J. Magn. Reson. 162 (2003) 90–101.
[23] T.D. Goddard, D.G. Kneller. SPARKY 3, University of California, San Francisco.
[24] M. Baldus, A.T. Petkova, J. Herzfeld, R.G. Griffin, Cross polarization in the tilted frame: assignment and spectral simplification in heteronuclear spin systems, Mol. Phys. 95 (1998) 1197–1207.
[25] A.E. Bennett, C.M. Rienstra, M. Auger, K.V. Lakshmi, R.G. Griffin, Heteronuclear decoupling in rotating solids, J. Chem. Phys. 103 (1995) 6951–6958.
[26] G. Bodenhausen, R. Freeman, G.A. Morris, Simple pulse sequence for selective excitation in Fourier-transform NMR, J. Magn. Reson. 23 (1976) 171–175.
[27] T. Nakai, C.A. McDowell, The necessity for synchronization in DANTE experiments with rotating samples—reclamation of the asynchronous DANTE pulse train by combination with the TOSS sequence, J. Magn. Reson. 90 (1990) 426–432.
[28] X.L. Wu, P. Xu, R. Freeman, A new kind of selective excitation sequence, J. Magn. Reson. 83 (1989) 404–410.